Effects of Electron Model on Three-Grid Ion Engine Analyses

IEPC-2011-205

Presented at the 32nd International Electric Propulsion Conference,
Wiesbaden • Germany
September 11 – 15, 2011

Takeshi Miyasaka[1] and Katsuo Asato[2]
Gifu University, Gifu, 501-1193, Japan

Fakhuradzi B. Baharudin[3]
Gifu University, Gifu, 501-1193, Japan

Hitoshi Sugiyama[4]
Gifu University, Gifu, 501-1193, Japan

and

Ikkoh Funaki[5]
JAXA, Sagamihara, Kanagawa, 229-8510, Japan

Abstract: To investigate the effects of the electron model in ion engine analysis, we carried out three-dimensional particle simulations using the full-PIC and hybrid PIC codes. Comparison of the results obtained using the two codes enabled us to understand the influence of the Boltzmann relation on the electric potential distribution. The results reveal that the number density of neutralizing electrons in the vicinity of the centerline of the hole downstream of a decel grid obtained using the hybrid-PIC code is higher than that obtained using the full-PIC code. The high number density of electrons in this region decreases the electric potential.

Nomenclature

e	=	elementary electric charge
k	=	Boltzmann constant
m_i	=	ion mass
m_e	=	electron mass
n_i	=	ion number density
n_e	=	electron number density
Te	=	electron temperature
w	=	axial velocity
ϕ	=	electric potential
ε_0	=	permittivity of free space

[1] Associate professor, Department of Human and Information Systems, miyasaka@gifu-u.ac.jp.
[2] Professor, Department of Human and Information Systems, asato@gifu-u.ac.jp.
[3] Graduate student, Department of Human and Information Systems, p3128027@edu.gifu-u.ac.jp.
[4] Graduate student, Department of Human and Information Systems, q3128014@edu.gifu-u.ac.jp.
[5] Associate professor, ISAS, funaki@isas.jaxa.jp.

I. Introduction

Ion engines are promising for use as space propulsion systems, and numerous experimental and numerical studies on ion engines have been carried out. The μ10 engine was used as the main engine of the asteroid probe Hayabusa.[1] Owing to their high specific impulse, ion engines are expected to be used in long-term mission satellites and probes. It is important to evaluate the engine lifetime for such long-term missions. However, real-time evaluation becomes increasingly difficult with increasing operation time. Therefore, methods for numerically predicting the lifetime are required. In previous numerical analyses of ion engines,[3-7] various types of models have been employed and the ion engine performance was predicted well.

To use numerical analysis as a tool for evaluating the engine lifetime, a code that predicts grid erosion quantitatively is required.[2] Grid erosion is caused by the impact of "collided ions" produced by collisions between neutrals and the constitutive part of the ion beam. Figure 1 shows a schematic of the impact of collided ions on the accel and decel grids. The tracking of ion motion and collisions enables us to estimate the rate of grid erosion (see Fig. 2). However, the calculation time becomes huge because three-dimensional analysis is required. In most codes, the electron number density is estimated from the Boltzmann relation. Because the Boltzmann relation is independent of the time step, which is determined by the characteristic speed of electrons, much higher than that of ions, the calculation cost is reduced. Thus, the Boltzmann relation is appropriate for three-dimensional analysis. However, the Boltzmann relation is a model for the electron number density distribution. Thus, the validity of the model should be confirmed before the quantitative evaluation of grid erosion.

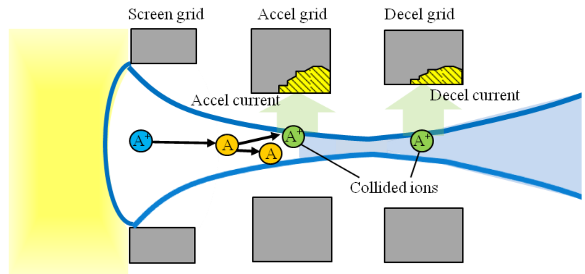

Figure 1. Schematic of impact of collided ions on accel and decel grids.

To investigate the applicability of the Boltzmann relation to the evaluations of grid erosion, we have been performing particle analyses on ion engines using full particle in cell (full-PIC) method,[8] in which ions and electrons are treated as particles.[9,10] In our previous studies,[9] analyses of the two-grid ion engines used in the experiments carried out by Hayakawa[11] were performed. The calculated grid currents agreed well with those obtained experimentally, and a characteristic erosion pattern referred to as "pits & grooves" was observed in the estimated erosion distribution of the downstream surface of the accel grid.

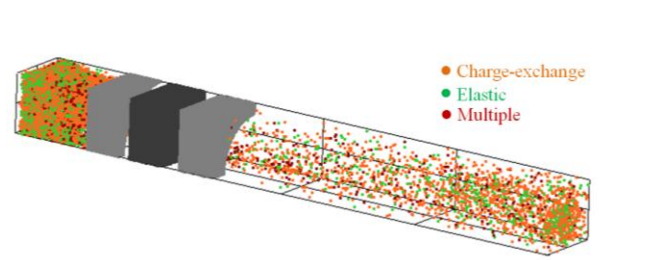

Figure 2. Distribution of collided ion particles.

In the present study, a full-PIC analysis of a Hayabusa type three-grid ion engine was carried out. To investigate the effect of the Boltzmann relation in three-grid ion engine analyses, a hybrid-PIC analysis using the Boltzmann relation was also performed. By the comparison of the electric potential distribution and the number density distribution of electrons obtained from the two analyses, the applicability of the Boltzmann relation to three-grid ion engines is discussed.

II. Numerical procedures

Full-PIC and hybrid-PIC analyses were performed with the same operational conditions and engine geometries. The propellant was assumed to be xenon. The following numerical procedures were applied in the present analyses (see Fig. 3).

A. Full-PIC analysis

The motion of charged particles is calculated by the full-PIC method. Both ions and electrons are treated as particles and move according to relative equations of motion. For the quantitative evaluations in this study, the 4th-order Runge-Kutta-Gill method is employed for the time integration of the equations of motion. The time step required for electron motion is much lower than that for ion motion, resulting in a huge calculation time. Thus, to shorten the calculation time, an artificial electron mass, assumed to be 10000 times smaller than the ion mass, is introduced. In past work,[10] it was found that for a ratio of ion mass to electron mass of higher than 10000, the electron distribution was nearly independent of the ratio.

Electric potential distributions are obtained by solving the Poisson equation by the FEM (finite element method).

$$\Delta\phi = -\frac{e(n_i - n_e)}{\varepsilon_0}. \tag{1}$$

The number densities of charged particles obtained by calculating the equation of motion are used in calculation of Eq. (1).

Elastic and charge-exchanged collisions between the ions constituting the ion beam and the neutrals are calculated. This analysis also treats multiple collisions between collided ions and neutrals. Owing to the high number density of neutrals compared with that of ions, the number density distribution of neutrals is fixed throughout the analyses. The distribution is calculated by the DSMC (direct simulation of Monte Carlo) method in advance. Because of the low ratio of the number density of collided ions to that of the ions constituting the ion beam, if a collision occurs, a collided ion and a collided neutral are added to the simulation.

B. Hybrid-PIC analysis

The numerical procedures in the hybrid-PIC analysis are almost the same as those in the full-PIC analysis except for the treatment of the electron motion. In the hybrid-PIC analysis, the number density distribution of electrons is estimated from the Boltzmann relation.

$$n_e = n_{e,ref}\exp\left\{\frac{e(\phi - \phi_{ref})}{kT_{e,ref}}\right\}. \tag{2}$$

The electric potential and electron number density of the plasma at the upstream boundary, ϕ_p and $n_{e,p}$, are used as the reference values $\phi_{p,ref}$ and $n_{e,ref}$ in Eq. (2), respectively. The electric potential and density of electrons, ϕ_e and $n_{e,e}$, at the downstream boundary are respectively used as $\phi_{p,ref}$ and $n_{e,ref}$ for the neutralizing electrons. In this study, ϕ_p and ϕ_e are 1510 and 0 V, respectively. The electric potentials on the screen grid, on the accel grid, and on the decel grid, ϕ_s, ϕ_A, and ϕ_D, are set to 1500, -400, and 0, respectively. By iterative calculation using Eqs. (1) and (2), self-consistent electric potential and electron number density distributions are obtained for the ion number density distribution obtained from the equation of motion.

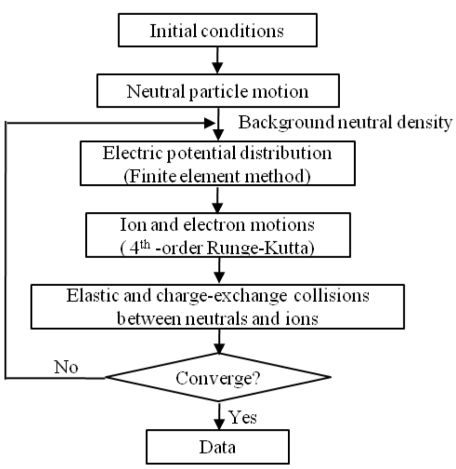

Figure 3. Schematic of numerical procedure

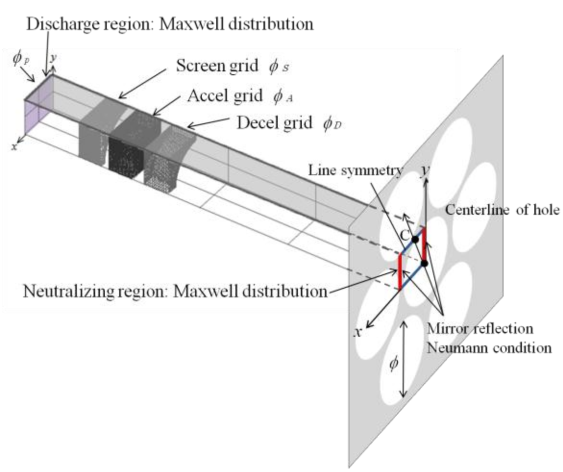

Figure 4. Schematic of three-dimensional calculation domain and conditions

C. Calculation domain and numerical conditions

The geometric parameters are chosen to be similar to those in the μ10 ion engine. To shorten the calculation time, the three-dimensional calculation domain is limited to a rectangular parallelepiped by applying some symmetry conditions, as shown in Fig. 4. Mirror reflection conditions are applied to the boundary surfaces except for the surface at $y = y_{max}$, where a line symmetry condition is applied. A rectangular grid with 43, 39, and 181 grid points in the *x*-, *y*-, and *z*-directions, respectively, is used. Uniform grid sizes are set in the *x*- and *y*-directions and a nonuniform grid size is set in the *z*-direction.

At the upstream boundary, the ion number densities of the plasma $n_{i,\,p} = n_{e,\,p}$ are applied. Electrons with the Maxwell distribution for a temperature of 5 eV and ions with a fixed axial velocity flow into the calculation domain. The ion number density of the plasma is determined from the beamlet current. In the present analyses, the beamlet current was set to 0.3 mA. On the downstream boundary surface, the number density of neutralizing electrons is set to the average ion density of the beamlet. Neutralizing electrons flow into the neutralizing region with the Maxwell distribution for a temperature of 5 eV.

III. Results and discussion

A. Electric potential and number density of electrons distributions

Figure 5 shows a comparison between the electric potential distributions at $y = 0$ mm obtained by the full-PIC and hybrid-PIC analyses. The two distributions agree well except for in the neutralizing region downstream of the decel grid. In the vicinity of the hole center and downstream of the decel grid, the electric potential for the full-PIC analysis is higher than that for the hybrid-PIC analysis. Figure 6 shows the electric potential distributions in the *x*-*y* plane along the white line shown in Fig. 5 for both analyses. In Fig. 6, a difference in the electric potential can be clearly observed. Figure 7 shows a comparison between the number density distributions of electrons at $y = 0$ mm obtained by the two analyses. The number density of electrons in the vicinity of the hole center and downstream of the decel grid for the full-PIC analysis is lower than that for the hybrid-PIC analysis. The difference can also be observed clearly in Fig. 8. These results indicate that the low number density in this region causes the high electric potential for the full-PIC analysis. Namely, in this region, the electric potential distribution is affected by the Boltzmann relation. The motion of ions is determined by the electric potential distribution. These results suggest that the Boltzmann relation may influence the rate of grid erosion.

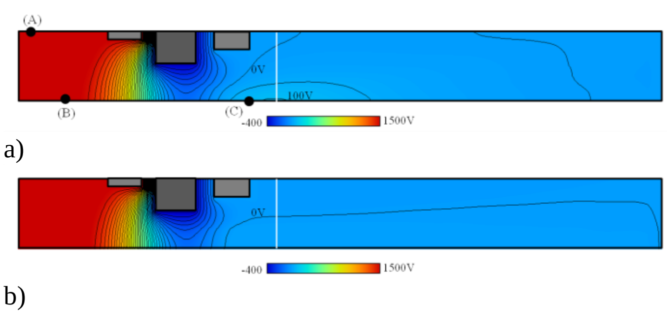

Figure 5. Two-dimensional distributions of electric potential (*y*=0) obtained by a) full-PIC analysis and b) hybrid-PIC analysis.

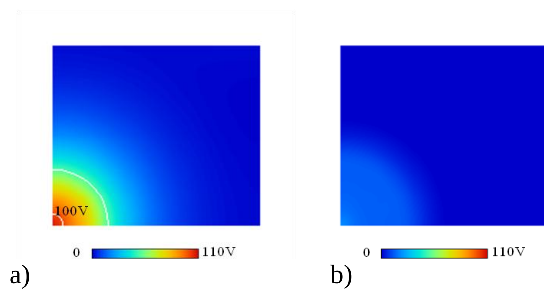

Figure 6. Two-dimensional distributions of electric potential along white line in Fig. 5 obtained by a) full-PIC analysis and b) hybrid-PIC analysis.

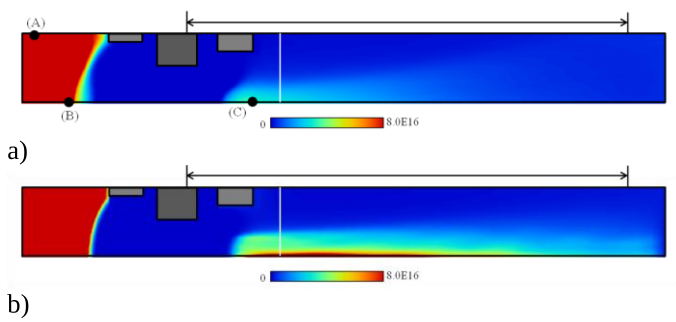

Figure 7. Two-dimensional distributions of electron number density (*y*=0) obtained by a) full-PIC analysis and b) hybrid-PIC analysis.

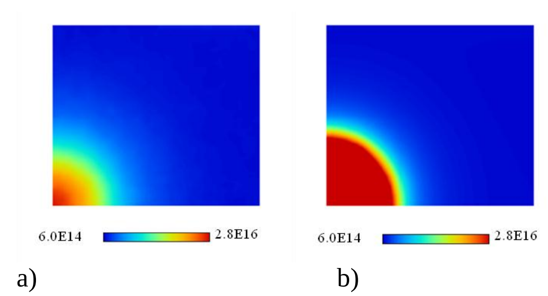

Figure 8. Two-dimensional distributions of electron number density along white line in Fig. 5 obtained by a) full-PIC analysis and b) hybrid-PIC analysis.

B. Velocity distribution of electrons

To investigate the difference between the distributions of the electron number density obtained by the full-PIC and hybrid-PIC analyses, the velocity distributions of electrons obtained by the full-PIC analysis were investigated. Figure 9 shows the calculated axial velocity distributions of electrons at points (A) and (B) in the upstream region, as shown in Figs. 5 and 7. Each distribution agrees well with the Maxwell distribution f, where

$$f = n_e \sqrt{\frac{m_e}{2\pi k T_e}} \exp\left(-\frac{\frac{1}{2} m_e w^2}{k T_e} \right). \tag{3}$$

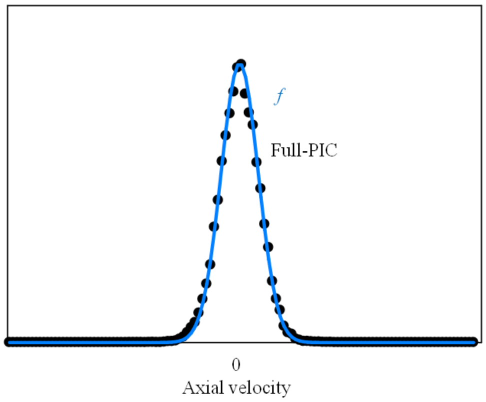

a)

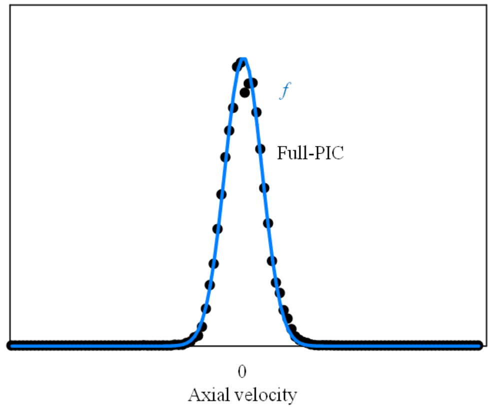

b)

Figure 9. Axial velocity distributions of electrons at a) (A) and b) (B) obtained by full-PIC analysis and velocity distributions *f*.

Figure 10 shows the axial distributions of the electron number densities and electric potentials along the centerline of the grid hole in the neutralizing region obtained by the two analyses (see Fig. 7). The number density distribution of electrons estimated from the Boltzmann relation for the electric potential obtained by the full-PIC analysis is also given in Fig. 10. The electron number density for the full-PIC analysis is much lower than that estimated from the Boltzmann relation. The axial velocity distribution of electrons at point (C) in Fig. 10, where the electric potential is higher than that on the boundary, is shown in Fig. 11. The distribution at (C) differs from the

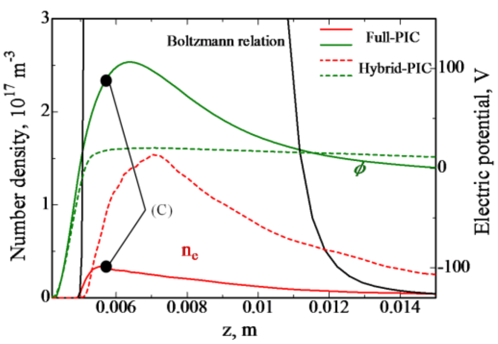

Figure 10. Axial distributions of ion and electron number densities and electric potentials along the centerline of the grid hole in the neutralizing region obtained by full-PIC and hybrid-PIC analyses.

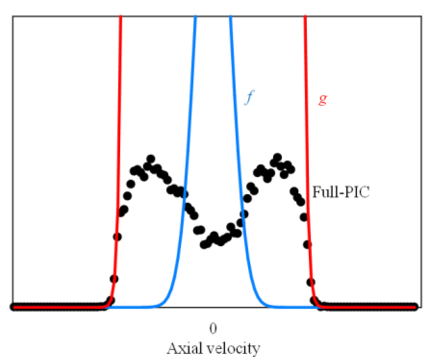

Figure 11. Axial velocity distribution of electrons at (C) obtained by full-PIC analysis and velocity distributions *f* and *g*.

Maxwell distribution *f*. The electrons flowing from the downstream boundary with the Maxwell distribution are accelerated by the positive difference between the electric potentials at (C) and at the boundary. Thus, the ratio of electrons in the low-velocity region decreases. Figure 11 reveals that the high ratio of electrons in the high-velocity region satisfies the velocity distribution including the effect of the difference between the electric potentials *g*, given by

$$g = n_{e,ref}\sqrt{\frac{m_e}{2\pi kT_e}}\exp\left\{-\frac{\frac{1}{2}m_e w^2 - e\left(\phi-\phi_{ref}\right)}{kT_e}\right\}. \tag{4}$$

The electric potential and electron number density for the hybrid analysis are self-consistent solutions of Eqs. (1) and (2). Because of the suppression of the positive electric potential in the neutralizing region, the electron number density for the hybrid-PIC analysis becomes low compared with that estimated from the Boltzmann relation using the electric potential in the full-PIC analysis. However, differences between the distributions of the electric potential and electron number density for the full-PIC and hybrid-PIC analyses are observed in Fig. 10.

IV. Conclusion

Differences between the electric potentials and electron number densities obtained by a full-PIC analysis and a hybrid-PIC analysis employing the Boltzmann relation were observed in the neutralizing region of a simulated three-grid ion engine. In this region, the electron number density obtained by the full-PIC analysis differs from that obtained using Boltzmann relation. This difference between the electron number densities is caused by the non-Maxwellian electrons in the positive-electric-potential region in the full-PIC analysis.

Acknowledgments

This work was supported by Japan Aerospace Exploration Agency under cooperative research project. The authors would like to thank members of the JIEDI (JAXA Ion Engine Development Initiatives) project for their supports.

References

[1]Funaki, I., Kuninaka, H. and Toki, K., "Plasma Characterization of a 10-cm Diameter Microwave Discharge Ion Thruster," *J. Propulsion and Power* , Vol. 20, No.4, 2004, pp.718-727.

[2]Kuninaka, H, "Research and Development of JIEDI (JAXA Ion Engine Development Initiatives) Tool for Numerical Evaluation of Ion Engine Grid Lifetime," *JAXA Special Publication*, JAXA-SP-06-019, pp.5-9, 2007 (in Japanese).

[3]Nakano, M, "Three-dimensional Simulations of Ion Engine Grid Erosion," *Advances in Applied Plasma Science*, Vol. 6, 2007, pp.93-96.

[4]Nakayama, N. and Wilbur, P.J., "Numerical Simulation of Ion Beam Optics for Multiple-grid Systems," *J. Propulsion and Power*, Vol. 19, No.4, 2003, pp.607-613.

[5]Wang, J., Cao, Y., Kafafy, R., Martinez, R., and Williams, J., "Ion Impingement Limits of Sub-Scale Ion Optics: Comparison of Simulation and Experiment," AIAA paper 2006-4999, 2006.

[6]Tartz, M., Hartmann, E., Deltschew, R., and Neumann, H., "Validation of a Grid Erosion Simulation by Short-time Erosion Measurements," Proceedings of the 26th International Electric Propulsion Conference, IEPC-99-147, 1999.

[7]Okawa, Y., Takegahara, H., "Particle Simulation on Ion Beam Extraction Phenomena in an Ion Thruster," *Proceedings of the 26th International Electric Propulsion Conference*, IEPC-99-146, 1999.

[8]Birdsall, C.K. and Langdon, A.B., *Plasma Physics via Computer Simulation*, MacGraw-Hill, 1985.

[9]Miyasaka, T, Kobayashi, T., and Asato, K., "Characteristics of Ions Impacting Grid Surfaces in an Ion Engine," *Vacuum*, Vol. 85, No. 5, 2010, pp.585-590.

[10]Miyasaka, T, Kobayashi, T., and Asato, K., "Numerical Prediction of Grid Erosion of Ion Engine," *Trans. of the Japan Soc. for Aeronautical and Space Sciences, Aerospace Technology Japan* [online journal], Vol. 8, No. ists27, 2010, pp.Pb_61-Pb_66, URL: http://www.jstage.jst.go.jp/browse/tastj/8/ists27/_contents/-char/ja/ [cited 9 March 2011].

[11]Hayakawa, Y., "Current Distribution on a Two-grid-ion-extraction-system Gridlet," *JAXA Special Publication*: JAXA-SP-06-019, pp.20-27, 2007 (in Japanese).